




# Synthesis and Analysis of Zirconium Titanate Thin Films by using Sol-Gel Method

Mohammad Hayath Rajvee <sup>1,\*</sup> , S.V. Jagadeesh Chandra <sup>2,\*</sup> , P. Rajesh Kumar <sup>1</sup>,  
CH.V.V. Ramana <sup>3,\*</sup>, Kalahasthi Neelama <sup>4</sup>, R. S. Dubey <sup>5</sup> 

<sup>1</sup> Department of Electronics and Communication Engineering, Andhra University College of Engineering (A), Andhra University, Visakhapatnam- 530003, Andhra Pradesh, India

<sup>2</sup> Department of Electronics and Communication Engineering, Vignan Institute of Information Technology, Duvvada, Visakhapatnam- 530049, Andhra Pradesh, India

<sup>3</sup> Department of Electrical and Electronics Engineering Science, Auckland Park Campus, University of Johannesburg, Johannesburg - 2006, South Africa

<sup>4</sup> Department of Electrical and Electronics Engineering, VB Institute of Technology, Hyderabad, Telangana, India.

<sup>5</sup> Advanced Research Laboratory for Nanomaterials and Devices, Department of Nanotechnology, Swarnandhra College of Engineering and Technology, Narsapur- 534280, West Godavari, Andhra Pradesh, India

\* Correspondence: razwe2003@gmail.com (M.H.R.); svjchandra@gmail.com (S.V.J.C.); ramana6@gmail.com (C.H.V.V.R.);

Scopus Author ID 57202051166

Received: 20.12.2020; Revised: 15.01.2021; Accepted: 18.01.2021; Published: 31.01.2021

**Abstract:** Titanium-doped zirconium oxide (mixed high-k) has been used as the gate oxide layer for the future generation metal oxide semiconductor devices. This mixed high-k layer was prepared by using Sol-Gel based spin-coated method. This mixed high-k layer's chemical, structural, and initial electrical properties are investigated thoroughly. It is clearly confirmed that the suitable chemical composition and bond formation of the proposed mixed high-k layer from EDAX and FTIR analysis observations. The XRD spectra strengthened the presence of ZrTiO<sub>2</sub>. The measured dielectric constant of the proposed mixed high-k layer from the extracted C-V plots has been varying from 29.1 to 37.6 with respect to spin coating from 4000 to 6000 rpm. With lower spin rates, the leakage current is less.

**Keywords:** zirconium titanate; ZTO; ULSI; gate capacitors; high-k dielectrics.

© 2020 by the authors. This article is an open-access article distributed under the terms and conditions of the Creative Commons Attribution (CC BY) license (<https://creativecommons.org/licenses/by/4.0/>).

## 1. Introduction

The chemical composition of a proposed mixed thin film will have a major role in achieving a metal oxide semiconductor device's enhanced performance. Though there was rigorous research on various high dielectric (high-k) TiO<sub>2</sub>, HfO<sub>2</sub>, Y<sub>2</sub>O<sub>3</sub>, La<sub>2</sub>O<sub>3</sub>, Gd<sub>2</sub>O<sub>3</sub>, Ta<sub>2</sub>O<sub>5</sub>, STO, ZrO<sub>2</sub>, Al<sub>2</sub>O<sub>3</sub> monolayers, recently there is an intensive focus on the mixed high-k layers to replace the SiO<sub>2</sub> [1-14] to have the bidirectional benefits on various physical and electrical applications. Among various high-k materials, TiO<sub>2</sub> has a wide range of applications due to its physical and chemical properties. Its applications extend as a photocatalyst, solar cell, electrochromic devices, anti-reflection coating, sensors. Besides, TiO<sub>2</sub> can also be used as reliable high-k material for DRAM applications because of its higher dielectric constant [15-17]. ZrO<sub>2</sub> has gained considerable attention during the recent decade because of its high bandgap of ~5eV [18], large melting and boiling points, high crystallization temperature, high thermal stability, high dielectric constant [19-20].

On the other hand, when we use these two high-k materials individually, there was a problem with the electronic instabilities of zirconium oxide on Si substrate. Eventually, there would be an unstable interface at  $\text{ZrO}_2/\text{Si}$  stacks [21-22], and  $\text{TiO}_2/\text{Si}$  shows a high leakage current even at low temperature due to a very low conduction band offset value [23]. To accumulate the benefits of both oxide layers at a stretch in a single device, we are proposing interface engineering to support the chemical configuration and physical structure of the titanium doped zirconium oxide ( $\text{ZrTiO}_2$ ) layers. Zr-doped  $\text{TiO}_2$  thin films can be prepared by Plasma-assisted pulsed laser deposited [24], and atomic layer deposition [25], electron beam evaporation, DC magnetron sputtering, RF magnetron sputtering, and chemical deposition methods, namely chemical bath deposition, chemical spray pyrolysis method [26], sol-gel spin coating method [1-3,19,27-28]. We have chosen a sol-gel spin coating method in this work because it is an inexpensive method; coating can be carried out at room temperature over large areas under atmospheric pressure. The amorphous nature of the film prepared through the sol-gel method, offers a very low leakage current of  $1.5 \times 10^{-6} \text{ A/cm}^2$ . Qian Zhang [1], and G. He *et al.*, [2] reported that the crystallization temperature could be raised to  $600^\circ\text{C}$  by incorporating titanium into zirconium. The incorporation of Zirconium into  $\text{TiO}_2$  offers an increase in the conduction band offset to Si and subsequently reduced the leakage current density by approximately two orders than pure  $\text{TiO}_2$  thin films.

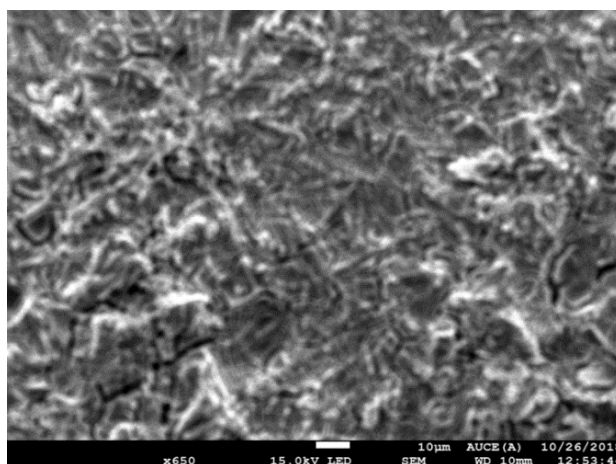
## 2. Materials and Methods

p-Type Si (100) wafers with a resistivity of 5-10 ohm-cm were used in this study. After removing the native oxide,  $\text{ZrTiO}_2$  films were deposited with a thickness of 40.0 nm, 41.20 nm, and 44.28 nm were grown on the wafers using sol-gel based spin-coating technique at 4000, 5000, and 6000 rpm for 30 Seconds with zirconium oxychloride octahydrate ( $\text{ZrOCl}_2 \cdot 8\text{H}_2\text{O}$ ) and titanium tetrachloride ( $\text{TiCl}_4$ ) precursors as the basic reactants. After each coating, the substrates were annealed at  $200^\circ\text{C}$  for 20 minutes. This process was repeated 10 times to achieve a considerable thickness of the coating. The physical thicknesses of the  $\text{ZrTiO}_2$  films were determined using ellipsometry studies. Thickness ( $t_{\text{ox}}$ ) and of the ZTO thin films have been measured with automatic angle spectroscopic ellipsometer [M2000VI] using multipoint measurement technique at the visible wavelength of 632.8 nm. Topographic analysis of the films is carried out using FESEM[JEOL JSM-7100F], and compositional analysis is done with OXFORD's EDX tool connected to FESEM. X-ray diffraction data were collected with a Philips x'pert system using  $\text{CuK}\alpha$  radiation ( $\lambda = 1.5418 \text{ \AA}$ ) at 45KV and step size of  $0.008^\circ$ .  $\text{TiCl}_4$  precursor was used as a dopant in the zirconium. A gel-like structure was formed upon the introduction of 2-Methoxy ethanol. All the chemicals were purchased from Sigma Aldrich (USA) and used without further purification or alteration. 0.62 grams of zirconium oxychloride octahydrate powder equivalent to 5 moles are mixed in 50ml of 2-methoxy ethanol using a magnetic stirrer for 5 min at 300rpm. Finally, 0.54 ml of titanium tetrachloride is added to the above mixture and again mixed by the magnetic stirrer for 720 min at 400 rpm. After stirring the  $\text{ZrTiO}_2$  solution for 12 hours, it was filtered using a  $0.22\mu\text{m}$  syringe filter to get a clear transparent solution.

All the as-deposited  $\text{ZrTiO}_2$  films were baked treated for 2 hrs at  $200^\circ\text{C}$ . After metallization (Contacts on both sides), though e-Beam evaporation, the samples are loaded into the furnace for baking at  $200^\circ\text{C}$  for 2hrs Al/ $\text{ZrTiO}_2$ /p-Si gate capacitor.

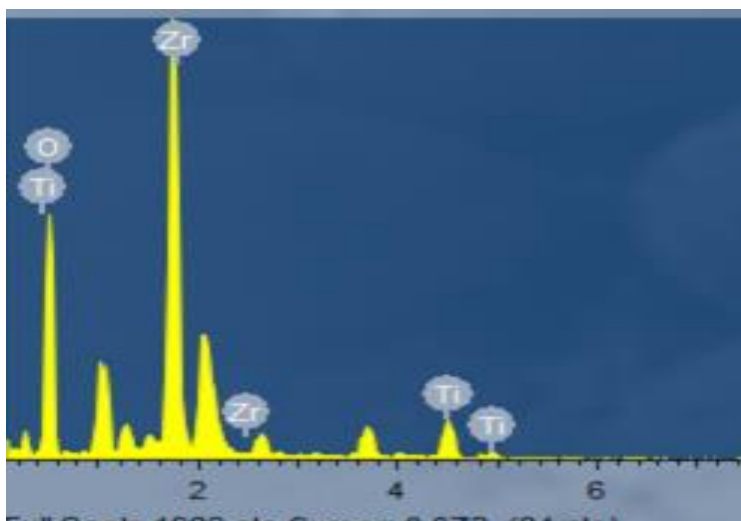
### 3. Results and Discussion

Figure 1 shows the field emission scanning electron micrograph of the films formed at 4000 rpm. The film's topography showed a uniform coating made with the spin coating with less porosity and negligible cracks and delaminations on its surface. The other films formed at 5000 and 6000 rpm (not shown here) also showed similar topography. Image is taken from FESEM at 650x magnification; over a surface of 10 $\mu$ m. FESEM enables obtaining chemical information from the specimen by using various techniques, including the X-ray energy dispersive spectrometer (EDS).



**Figure 1.** FESEM image of ZrTiO<sub>2</sub> Thin Film.

The EDS spectrum, shown in figure 2. It has been obtained from FESEM through oxford's EDX attachment connected to it. The highest peak is shown in the spectrum shown as zirconium with 6.68 Weight%. The titanium quantity is approximately half of zirconium, confirming the 1:2 molar ratio of titanium and zirconium. The quantity of oxygen (shown in table 1), is more because it contains oxygen in the thin film, substrate silicate oxygen, and film surface. The Quantitative representation of materials in the oxide layer is shown in Figure 3. EDX data is collected at a working distance of 10mm, a probe current of 8mA, and a maintained accelerating voltage of 10KV. The numerical representation of the available major elements is shown in table 1.



**Figure 2.** EDX Spectrum of ZrTiO<sub>2</sub> Thin film.

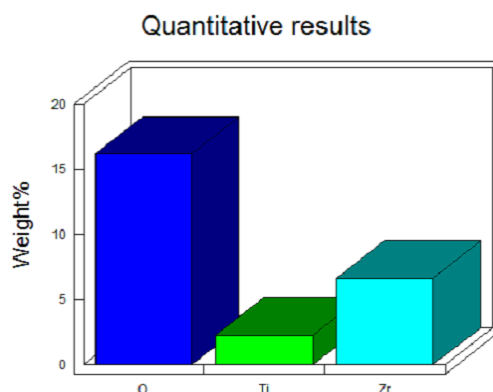


**Figure 3.** Bar-Chart of ZrTiO<sub>2</sub> Thin film.

**Table 1.** Elemental composition of ZrTiO<sub>2</sub>

Element	Weight%	Atomic%
O K	16.2	89.34
Ti K	2.28	4.20
Zr K	6.68	6.46
Totals	25.16	-

Figure 4 shows the FTIR spectrum of ZrTiO<sub>2</sub> films. The X-axis represents the wavelength (cm<sup>-1</sup>), and Y-axis represents light absorbance passing through the sample. The band at 2744cm<sup>-1</sup> indicating a vibration Zr-O bond. The bond at 3700 cm<sup>-1</sup> corresponds to the vibration of the Si-O bond. The band stretching in the range 2060-3600 cm<sup>-1</sup> was attributed to a surface hydroxyl group's symmetrical vibration. A broad absorption seen in the range 3100-3700 cm<sup>-1</sup> might be related to the stretching hydroxyl (O-H) group resulting from titanium isopropoxide hydrolysis. Carbon-based functionalization traces identified on pure Zr doped TiO<sub>2</sub> surface may reflect between 1600-2100 cm<sup>-1</sup>. The band at 1640 cm<sup>-1</sup> representing the O-H bending mode of the absorbed water. The band at 2360 cm<sup>-1</sup> is because of the absorbed water (H<sub>2</sub>O) molecules after sol-gel coating.

The bands in the range 950-400 cm<sup>-1</sup> can be assigned to different stretching modes associated with metal oxides. In our case, the band may be attributed to the Ti-O bands in Zr-doped TiO<sub>2</sub> samples. The bands at 1242 cm<sup>-1</sup>, 1111 cm<sup>-1</sup>, 1035 cm<sup>-1</sup>, and 860 cm<sup>-1</sup> correspond to Ti-OH's vibration mode. The band around 665 cm<sup>-1</sup> was attributed to the vibration mode of the Ti-O-Ti bond; the most apparent peaks were observed at 443 cm<sup>-1</sup>, referring to the Ti-O-Ti stretching mode. FTIR spectrum of Figure 4 is enlarged and drawn in parts to show the low amplitude peaks clearly.

A search of the ICDD (International Centre for Diffraction Data) database of X-ray diffraction patterns enables the phase identification of a large variety of crystalline samples. The  $\theta$ -2 $\theta$  scan maintains these angles with the sample, detector, and X-ray source. Only those planes of atoms that share this normal will be seen in the  $\theta$ -2 $\theta$  scan. The inter-planar distance can be calculated from Bragg's law substituting  $\lambda$  and  $\theta$  values from the XRD results,

$$D_p = 0.94 \lambda / \beta \cos \theta$$

Where  $\beta$  = Line broadening in radius

$\lambda$  = wavelength of characteristic X-rays (1.540Å)

$\theta$  = Bragg's angle,

$D_p$  = Average crystal size

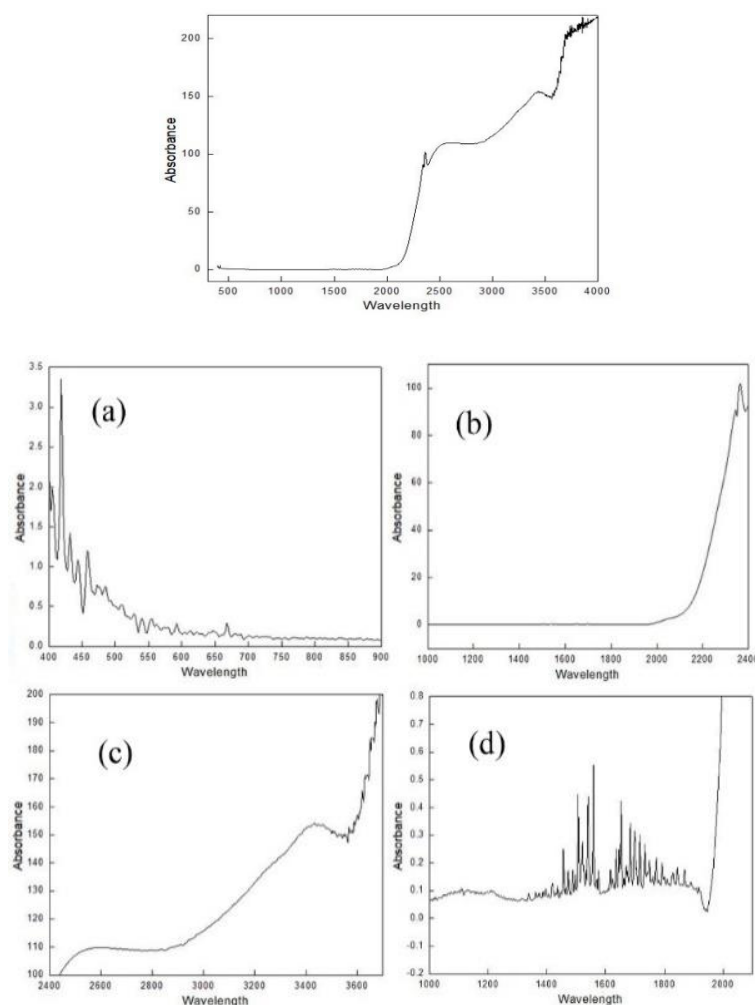


**Figure 4.** FTIR spectrum of ZrTiO<sub>2</sub>.

The XRD pattern of titanium doped ZrO<sub>2</sub> in Figure 5 shows a smooth line without any specific peaks. The absence of peaks indicates the amorphous nature of the material. The amorphous nature is more suitable for MOS capacitor applications. XRD patterns of ZrTiO<sub>2</sub> thin film are the same for 4000, 5000, and 6000 rpm, and crystalline size is 22 nm.

C-V measurements carried out by using the Agilent (model:1500A) Semiconductor Device Analyzer taken at 100 kHz are plotted in Figure 6. Three regions of the C-V graph, namely accumulation, depletion, and inversion, formed due to variation in carrier concentrations at the interface with bias voltage, are distinctly visible. The maximum accumulated capacitance is found to be 511 pF at 4000 rpm, 132 pF at 5000 rpm, and 183 pF at 6000 rpm. The dielectric constant calculated from the C-V plot was 37.6, 32.1, and 29.1, respectively, for samples at spin rates of 4000 rpm, 5000 rpm, and 6000 rpm.

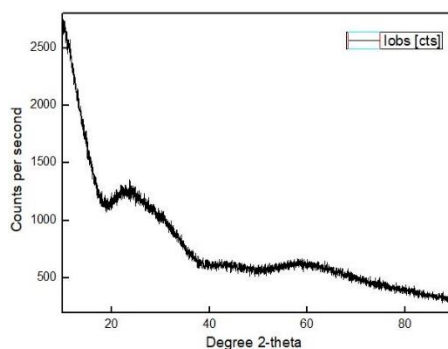


**Figure 5.** XRD image of ZrTiO<sub>2</sub> Thin Film.

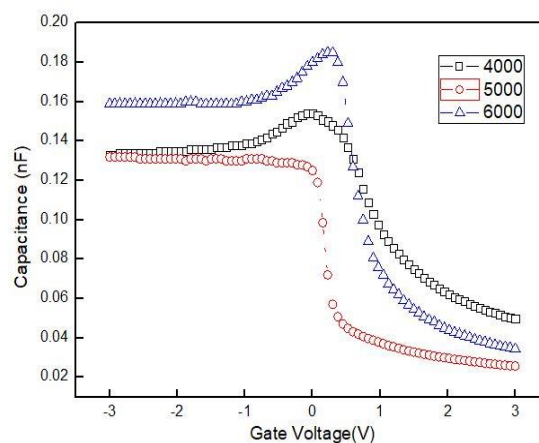


**Figure 6.** C-V analysis of ZrTiO<sub>2</sub> thin film.

This dielectric constant variation is attributed to the variations of oxide layer thickness because of different spin rates adopted. Oxide layer thickness varies from 44 nm to 40 nm. The maximum gate leakage current is 152 nA for 4000 rpm, 26.7 nA for 5000 rpm, and 369 nA for 6000 rpm, which is lower than that of the existing literature and consistent for the use in MIS structures. All the parameters are shown in table number 2. Overshoot in the CV graph is observed against the 6000 rpm curve because of the excessive trap charges available at the interface.

The conductivity of the prepared ZrTiO<sub>2</sub> solution is measured using an electrical conductivity meter. We aim to prepare a solution, which is a purely insulating material. Generally, the insulating material's conductivity value is greater than or equal to  $10^{-8}$  S/cm. The conductivity value of the prepared ZrTiO<sub>2</sub> solution is  $10^{-8}$  S/cm. Electrical Conductivity Meter gives only the magnitude and not a graph. Table 2 shows a summary of the results.

**Table 2.** Result summary.

	Thickness ( $t_{ox}$ )	Refractive Index ( $n$ )	Maximum Accumulation Capacitance $C_{max}$	Dielectric constant ( $k$ )	EOT	Flatband Voltage ( $V_{fb}$ )	Bandgap	Maximum Leakage Current at +2V
4000 rpm	44nm	1.86562	1.52E-10	37.6	4.5nm	0.375V	4.2	152nA
5000 rpm	41.203nm	1.77468	1.32E-10	32.1	5nm	0.1V	4.3	26.7nA
6000 rpm	40.381nm	1.27867	1.83E-10	29.1	5.4nm	-0.3V	4.4	369nA

## 4. Conclusions

The primary focus of this work is to study the electrical characteristics of the high-k dielectric layer of Zirconium Titanate (ZrTiO<sub>2</sub>) prepared using Sol-Gel based spin coating technique. Initially, titanium doped zirconium dioxide solution is prepared using the Sol-Gel method; after preparation of the solution, it is tested for conductivity, which is  $10^{-8}$  siemens/cm. This confirms the prepared material's suitability to be used as a dielectric material. The solution is then deposited on glass substrates and p-Si(100) using the spin coating method at varying speeds of 4000, 5000, and 6000 rpm. The films are characterized for their chemical, structural and electrical properties. From the XRD graph, it is known that the prepared films are purely amorphous. From the FESEM results, the thin film morphology is found to be smooth, and a uniform deposition had taken place. From the EDX results, the Zr:Ti ratio is shown as 1:2. The thickness of the thin film is obtained by characterizing the film using a spectroscopic ellipsometer.

Film thicknesses were 44, 41, and 40 nm respectively for 4000, 5000, and 6000 rpm spin rates. Thus it satisfies the relation, i.e., the spin speed is inversely proportional to the film



thickness. Obtained Leakage currents are much lower than the reported gate leakage current density. The values obtained from Agilent 1500A Semiconductor Device Analyzer are 152 nA, 26.7 nA, and 369 nA, respectively, for different spin rates. Maximum accumulation capacitance ( $C_{\max}$ ) values are 15.2 nF, 13.2 nF and 18.3 nF. Calculated dielectric constant( $k$ ) values from the accumulation capacitance are 37.6, 32.1, and 29.1, respectively, for three different spin rates. These values are greater than the reported values.

## 5. Future Scope

The deposited films can be annealed at various temperatures like 400°C, 500°C, and 600°C to analyze the MOSCAP device properties like dielectric constant, leakage current, and equivalent oxide thickness based on the changes in crystal orientation of the material (phase formation).

## Funding

This research received no external funding.

## Acknowledgments

This research has no acknowledgment.

## Conflicts of Interest

The authors declare no conflict of interest.

## References

1. Zhang, Q.; Guodong, X.; Wenwen, X.; Ji, Z.; Sumei, W. Low-temperature solution-processed high- $k$  ZrTiO<sub>x</sub> dielectric films for high-performance organic thin film transistors. *Applied Physics* **2015**, *79*, 182-911. <https://doi.org/10.1016/j.synthmet.2015.10.011>.
2. Xia, D.Q.; He, G.; Liu, M.; Gao, J.; Jiang, S.S.; Li, D.; Zhang, M.; Liu, Y.M.; Lv, J.G.; Sun, Z.Q. Modification of optical and electrical properties of sol-gel-derived TiO<sub>2</sub>-doped ZrO<sub>2</sub> gate dielectrics by annealing temperature. *Journal of Alloys and Compounds* **2016**, *688*, 252-259, <https://doi.org/10.1016/j.jallcom.2016.07.179>.
3. Rabah, B.; Hanene, B. Synthesis, Characterization and properties of Zirconium oxide doped Titanium oxide thin films obtained via sol-gel process. *Heat Treatment Conventional Applications* **2015**, *95*, 22-26, <https://doi.org/10.5772/51155>.
4. Kondaiah, P.; Jagadeesh Chandra, S.V.; Fortunato, E.; Jong, C.H.; Mohan Rao, G.; Reddy, D.V.R.K.; Uthanna, S. Substrate temperature influenced ZrO<sub>2</sub> films for MOS devices. *Surface and Interface Analysis* **2020**, *52*, 541-546, <https://doi.org/10.1002/sia.6775>.
5. Kumar, N.M.; Jagadeesh Chandra, S.V.; Ju, M.; Dutta, S.; Ramana, C.H.V.V.; Qamar, H.S.; Park, J.; Kim, Y.; Cho, Y.H.; Cho, E.C.; Yi, J. Influence of ultra-thin Ge<sub>3</sub>N<sub>4</sub> passivation layer on structural, interfacial and electrical properties of HfO<sub>2</sub>/Ge metal oxide semiconductor devices. *Journal of Nanoscience and Nanotechnology* **2020**, *20*, 1039-1045, <https://doi.org/10.1166/jnn.2020.16934>.
6. Kumar, M.; Jagadeesh Chandra, S.V.; Ju, M.; Dutta, S.; Swagata, P.; Sanyal, S.; Pham, D.P.; Qamar, S.H.; Kim, Y.; Park, J.; Cho, Y.H.; Cho, E.C.; Yi, J. Effects of post deposition annealing atmosphere on interfacial and electrical properties of HfO<sub>2</sub>/Ge<sub>3</sub>N<sub>4</sub> gate stacks. *Thin Solid Films* **2019**, *675*, 16-22, <https://doi.org/10.1016/j.tsf.2019.02.034>.
7. Janardhanam, V.; Yun, H.J.; Jyothi, I.; Yuk, S.H.; Lee, S.N.; Won, J.; Choi, C.J. Fermi-level depinning in metal/Ge interface using oxygen plasma treatment. *Applied Surface Science* **2019**, *463*, 91-95, <https://doi.org/10.1016/j.apsusc.2018.08.187>.
8. Reddy, P.R.S.; Janardhanam, V.; Lee, H.K.; Shim, K.H.; Lee, S.N.; Reddy, V.R.; Choi, C.J. Schottky barrier parameters and low-frequency noise characteristics of Au/Ni contact to n-type  $\beta$ -Ga<sub>2</sub>O<sub>3</sub>. *Journal of Electronic materials* **2020**, *49*, 297-305, <https://doi.org/10.1007/s11664-019-07728-z>.

9. Rashid, H.; Rahman, K.S.; Hossain, M.I.; Nasser, A.A.; Alharbi, F.H.; Akhtaruzzaman, M.; Amin, N. Physical and electrical properties of molybdenum thin films grown by DC magnetron sputtering for photovoltaic application. *Results in Physics* **2019**, *14*, <https://doi.org/10.1016/j.rinp.2019.102515>.
10. Shukor, A.H.; Alhattab, H.A.; Takano, I. Electrical and optical properties of copper oxide thin films prepared by DC magnetron sputtering. *Journal of Vacuum Science & Technology* **2020**, *B38*, <https://doi.org/10.1116/1.5131518>.
11. Dewi, R.K.; Zuhdi, Z.; Hussain, T.S.L. Analysis of optical and electrical properties of thin films Ba<sub>1-x</sub>Sr<sub>x</sub>RiO<sub>3</sub> (with x=0.1 and x = 0.6). *International Journal of Advanced Science and Technology* **2020**, *29*, 365–377, <http://sersc.org/journals/index.php/IJAST/article/view/3922>.
12. Chen, X.; Yu, Z.; Guan, X.; Hao, Z. Facile synthesis of Solution-processed Silica and Polyvinyl phenol hybrid dielectric for flexible organic transistors. *Nanomaterials* **2020**, *10*, <https://doi.org/10.3390/nano10040806>.
13. Devesa, S.; Teixeira, S.S.; Rooney, A.P.; Graca, M.P.; Cooper, D.; Costa, L.C. Structural, morphological and dielectric properties of ErNbO<sub>4</sub> prepared by the Sol-Gel method. *Journal of Physics and Chemistry of Solids* **2020**, <https://doi.org/10.1016/j.jpcs.2020.109619>.
14. Hwang, D.; Shin, S.; Kim, H.; Lee, T. A study on improvement of optical/electrical properties of Indium-tin oxide thin films prepared by Sol-Gel process. *SAE Technical paper* **2019**, <https://doi.org/10.4271/2019-01-0187>.
15. Chandra Sekhar, M.; Kondaiah, P.; Jagadeesh Chandra, S.V.; Mohan Rao, G.; Uthanna, S. Effect of substrate bias voltage on the structure, electric and dielectric properties of TiO<sub>2</sub> thin films by DC magnetron sputtering. *Applied Surface Science* **2011**, *258*, 1789–1796, <https://doi.org/10.1016/j.apsusc.2011.10.047>.
16. Zhu, H.E.; Zhao, B.; Liu, X.; Kang, J.; Han, R. Fabrication and Electrical Properties of Titanium Oxide by Thermally Oxidizing Titanium on Silicon. *Chinese Journal of Semiconductors* **2002**, *23*, 337-341.
17. Chandra Sekhar, M.; Kondaiah, P.; Mohan Rao, G.; Jagadeesh Chandra, S.V.; Uthanna, S. Post-deposition annealing influenced structural and electrical properties of Al/TiO<sub>2</sub>/Si gate capacitors. *Super lattices and Microstructures* **2013**, *62*, 68–80, <https://doi.org/10.1016/j.spmi.2013.07.001>.
18. Sue-Min, C.; Ruey-An, D. Inter band Transitions in Sol-Gel-Derived ZrO<sub>2</sub> Films under Different Calcination Conditions. *American Chemical Society* **2007**, *49*, 501-520. <https://doi.org/10.1021/cm070606n>.
19. Ramalingam, S. Synthesis of nanosized Titanium dioxide by Sol-Gel technique. *International journal of Innovative Technology and Exploring Engineering (IJITEE)* **2019**, *9*, 732-735, <https://doi.org/10.35940/ijitee.B1174.1292S219>.
20. Ganesh, S.; Sang, Y.K. High-k polymer nanocomposite materials for technological applications. *Applied sciences* **2020**, *10*, 4249-4267, <https://doi.org/10.3390/app10124249>.
21. Akkaya, A.; Boyarbay, B.; Cetin, H.; Yildizli, K.; Ayyildiz, E. A study on the electronic properties of SiO<sub>x</sub>Ny/p-Si interface. *Silicon* **2018**, *10*, 2717-2725, <https://doi.org/10.1007/s12633-018-9811-6>.
22. Amit, K.; Shailey, S.; Shilpi, A.; Rajendra, P.B.; Sharma, A.K. Influence of Synthetic Approach of SiO<sub>2</sub>-ZrO<sub>2</sub> Materials. *Catal. Sustain. Energy* **2018**, *5*, 34–40, <https://doi.org/10.1515/cse-2018-0005>.
23. Venkataiah, S.; Jagadeesh Chandra, S.V.; Chalapathi, U.; Ramana, C.H.V.V.; Uthanna, S. Oxygen partial pressure influenced stoichiometry, structural, electrical and optical properties of DC reactive sputtered hafnium oxide films. *Surface and Interface Analysis* **2020**, 1-9, <https://doi.org/10.1002/sia.6902>.
24. Ogugua, S.N.; Martin, O.N.; Swart, H.C. Latest development on pulsed laser deposited thin films for advanced luminescence applications. *Coatings* **2020**, *10*, 1078-1100, <https://doi.org/10.3390/coatings10111078>.
25. Xin, W.; Ghosh, S.K.; Mohajer, M.A.; Hua, Z.; Yongqiang, L.; Xiaoxiao, H.; Jiyu, C.; Min, Z.; Xiangbo, M. Atomic layer deposition of Zirconium oxide thin films. *Journal of Materials Research* **2020**, *35*, 804-812, <https://doi.org/10.1557/jmr.2019.338>.
26. Oluwabi, A.T.; Juma, A.O.; Acik, I.O.; Arvo, M.; Malle, K. Effect of Zr doping on the structural and electrical properties of spray deposited TiO<sub>2</sub> thin films. *Proceedings of the Estonian Academy of Sciences* **2018**, *67*, <https://doi.org/10.3176/proc.2018.2.05>.
27. Kayani, Z.N.; Anum, K.; Zeb, S.; Saira, R.; Shahzad, N. Probe of ZrTiO<sub>2</sub> thin films with TiO<sub>2</sub>-ZrO<sub>2</sub> binary oxides deposited by dip coating technique. *Journal of Photochemistry and Photobiology B: Biology* **2018**, *183*, 357-366, <https://doi.org/10.1016/j.jphotobiol.2018.04.051>.
28. Rajvee, M.H.; Kumar, P.R.; Srinivasarao, Y. Effect of pre synthesis sintering on bandgap of CeZrO<sub>4</sub> nano crystalline powders prepared through high energy ball milling for high k dielectric thin films. *2018 Conference on Signal Processing And Communication Engineering Systems (SPACES)* **2018**, <https://doi.org/10.1109/SPACES.2018.8316334>.